Quantitative Analysis of Herpes Simplex Virus Reactivation In Vivo Demonstrates that Reactivation in the Nervous System Is Not Inhibited at Early Times Postinoculation

N. M. Sawtell*

Division of Infectious Diseases, Children's Hospital Medical Center, Cincinnati, Ohio 45229-3039

Recent studies utilizing an ex vivo mouse model of herpes simplex virus (HSV) reactivation have led to the hypothesis that, under physiologic conditions inducing viral reactivation, the immune cells within the infected ganglion block the viral replication cycle and maintain the viral genome in a latent state. One prediction from the ex vivo study is that reactivation in ganglia in vivo would be inhibited at early times postinoculation, when the numbers of inflammatory cells in the ganglia are greatest. To distinguish between an effect of the immune infiltrates on (i) infectious virus produced and/or recovered in the ganglion and (ii) the number of neurons undergoing lytic transcriptional activity (reactivating), an assay to quantify the number of neurons expressing lytic viral protein in ganglia in vivo was developed. Infectious virus and HSV protein-positive neurons were quantified from days 9 through 240 postinoculation in latently infected trigeminal ganglia before and at 22 h after hyperthermic-stress-induced reactivation. Significant increases in the amount of virus and the number of positive neurons were detected poststress in ganglia at all times examined. Unexpectedly, the greatest levels of reactivation occurred at the times examined most proximal to inoculation. Acyclovir was utilized to stop residual acute-phase virus production, and this treatment did not reduce the level of reactivation on day 14. Thus, the virus measured after induction was a product of reactivation. These data indicate that, in contrast to observations in the ex vivo model, immune cells in the ganglia during the resolution of acute infection do not inhibit reactivation of the virus in ganglia in vivo.

Herpes simplex virus (HSV) invades the host nervous system during infection at the body surface (7, 38, 40, 44; for a review, see reference 8). In the nervous system, the virus proceeds through the lytic replicative cycle in some neurons, whereas in others lytic-phase transcription is either not initiated or aborted and the viral genome enters a transcriptionally repressed or latent state (see reference 31 for a recent review). These latently infected neurons serve as a lifelong reservoir of viral genetic information within the host. Periodically, in response to stressful stimuli, there is reentry into lytic-phase transcription and infectious virus is produced. This virus is amplified and shed at the surface, either asymptomatically or in association with lesions.

In animal models and in humans, HSV reactivation occurs despite an activated competent immune response. Although several potential strategies for immunoevasion by HSV have been identified (discussed in references 1, 19, and 24), which, if any, of these strategies are important for recurrent disease and transmission remains unclear. There is evidence in animal models that augmenting the immune response by specific immunotherapeutic strategies can reduce peripheral disease associated with reactivation (13, 14, 28, 30, 47, 48). Theoretically, immunotherapeutic strategies could function to block or reduce reactivation at several stages, including (i) prior to significant viral protein expression in the neuron stimulated to reactivate, (ii) after the onset of lytic viral transcriptional activity but prior to the release of infectious virus, or (iii) after virus was produced in the ganglion but before the onset of significant replication at the surface. Studies to date have focused exclusively on the end stages of reactivation, i.e., viral replication or lesions at the body surface, and thus the stage at which the heightened immune response exerts an effect on the disease process is not clear. Recently, evidence that CD8+ T cells resident in ganglia at 14 days postinoculation can block HSV reactivation from latency in an ex vivo model was reported (21) and, further, it has been reported that this effect was at least in part due to gamma interferon (20). It was also shown that the ability of the immune cells in the ganglia to block ex vivo reactivation waned as the time postinfection (p.i.) increased (21). Combined, these studies suggest that immune augmentation strategies may be exploited to block or reduce HSV reactivation early in the process, i.e., in the ganglion.

A first step toward addressing this issue was to determine whether, as suggested by the ex vivo studies of Hendricks and coworkers (20, 21), reactivation is indeed decreased at early times p.i. in vivo. In the present study, the efficiency of HSV reactivation from days 9 through 240 p.i. was determined. Reactivation was quantified in three ways: (i) the number of ganglion undergoing reactivation, (ii) the amount of virus recovered per reactivating ganglion, and (iii) the number of neurons undergoing reactivation per reactivating ganglion. In order to quantify the number of neurons reactivating, a whole-tissue immunohistochemical (IHC) approach for the analysis of viral protein expression during latency and after a reactivation stimulus was developed and validated. This assay, combined with a quantitative analysis for the amount of infectious virus in the ganglia at the time of peak virus production postin-

* Mailing address: Division of Infectious Diseases, Children's Hospital Medical Center, 3333 Burnet Ave., Cincinnati, OH 45229-3039. Phone: (513) 636-7880. Fax: (513) 636-7655. E-mail: sawtn0@chmcc.org.

duction, clearly demonstrated that reactivation in vivo is not impaired at times of maximum immune cell infiltrate.

MATERIALS AND METHODS

Viral strains and stock production. Virus stocks of laboratory strain 17syn+ were generated by routine propagation on rabbit skin cell monolayers (RSC) (38). Infected cells were harvested and sonicated, and the titer of each stock was determined by serial-dilution plaque assay on RSC monolayers. The wild-type HSV type 1 strain 17syn+ was originally obtained from John H. Subak-Sharpe at the Medical Research Council Virology Unit in Glasgow, Scotland.

Inoculation of mice. All procedures involving animals were approved by the Children's Hospital Institutional Animal Care and Use Committee and were in compliance with the *Guide for the Care and Use of Laboratory Animals*. Animals were housed in American Association for Laboratory Animal Care-approved quarters. Male, outbred, Swiss-Webster mice (Harlan Laboratories), 4 to 5 weeks of age, were used throughout these studies. Prior to inoculation, mice were anesthetized by intraperitoneal injection of sodium pentobarbital (Nembutal [50 mg/kg of body weight]). A 10-μl drop containing 10^5 PFU was placed onto each scarified corneal surface. In our laboratory, this inoculum titer results in ~80% survival of mice with 100% of ganglia latently infected.

ACV treatment. Acyclovir (ACV; Glaxo-Wellcome) was dissolved in 0.15 M sterile saline at 5 mg/ml just before use. Doses of 50 mg/kg of body weight were administered by intraperitoneal injection to mice at 8-h intervals as indicated in Results.

Replication in vivo. In order to confirm the efficiency of inoculation and progression of acute infection, three mice from each inoculation group were sacrificed on days 2, 4, 6, 8, and 10 p.i. Eyes and trigeminal ganglia (TG) were removed and assayed for infectious virus titer by serial dilution on RSC monolayers.

In vivo reactivation. HSV was induced to reactivate in the ganglia of mice in vivo by using hyperthermic stress (HS). This procedure has been described in detail previously (38). In brief, mice were placed into restrainers, suspended in a 43°C water bath for 10 min, and subsequently towel dried and placed in a 37°C incubator to prevent hypothermia. At the indicated times posttreatment, mice were euthanized, and the TG were removed and homogenized individually on ice in minimal essential medium containing 5% newborn calf serum. After centrifugation to pellet cellular debris, the entire homogenate (~1.5 ml) from each ganglion was placed onto a 60-mm RSC monolayer and absorbed for 2 h with gentle rocking at 37°C in a 5% CO_2 incubator. Plates were then rinsed with medium and overlaid with medium containing 1% carboxymethyl cellulose. Plaques appeared within 24 to 48 h postplating. For quantification of plaques, the carboxymethyl cellulose overlay was removed from the plates, which were then rinsed in phosphate-buffered saline (PBS) and stained with crystal violet. Plaques were counted under a dissecting microscope.

Antibodies and WGIHC. Immunohistochemistry (IHC) on whole-ganglia IHC (WGIHC) was carried out with modifications of a procedure previously reported by Luque et al. (25).

Tissue collection. Perfusion fixation and drop fixing work equally well with this procedure. In most studies reported here, one ganglion from a mouse was used for the detection of infectious virus, and the other was used for the detection of viral protein; therefore, drop fixation was performed. Mice were euthanized, and the TG were rapidly removed and placed in the appropriate solution.

Fixation. Ganglia were fixed for 2 h in 0.5% paraformaldehyde, rinsed in PBS twice for 15 min, and then postfixed overnight in methanol containing 20% dimethyl sulfoxide (DMSO). All of the fixation, rinsing, and incubation steps were performed with continuous gentle mixing by placing the tubes containing tissue on a Nutator (Adams).

Treatment for endogenous peroxidase activity. Ganglia were incubated for 1 h in a solution of methanol containing 20% DMSO and 10% H_2O_2. After two 15-min rinses in 100% methanol, ganglia were stored overnight in methanol at −70°C. Ganglia are allowed to equilibrate at room temperature for 15 min, rinsed twice in PBS, and incubated for 2 h at 37°C in PBS containing 3.6 mg of β-D-(+)glucose (Sigma)/ml, 100 μg of glucose oxidase (Sigma)/ml, and 130 μg of sodium azide (Mallinckrodt)/ml.

Incubation with primary antibody. Ganglia were rinsed twice in PBS and incubated overnight at 37°C in the primary antibody, rabbit anti-HSV type 1/2 (Accurate) diluted 1:3,000 in PBS containing 2% bovine serum albumin, 5% DMSO, and 5% normal horse serum.

Incubation with HRP conjugate. After a rinse for 5 h, which included five changes of PBS, ganglia were incubated overnight at room temperature in a 1:500 dilution of anti-rabbit horseradish peroxidase (HRP) conjugate (Vector) diluted in PBS containing 2% bovine serum albumin, 5% DMSO, and 5%

normal horse serum. The tissue samples were again rinsed in PBS, with five changes over a period of 5 h, followed by a final rinse in 0.05 M Tris-Cl (pH 8.2).

Color development. Ganglia were then incubated in a solution containing 250 μg of diaminobenzidine (Aldrich)/ml and 0.004% H_2O_2 in 0.1 M Tris (pH 8.2). The reaction was carefully monitored by visualizing color development and stopped by rinsing in distilled H_2O. Rinsed ganglia were either cleared in glycerol and mounted between two glass slides or processed for routine IHC as described below.

Note. Care must be taken to avoid including any pieces of lacrimal gland with the ganglia. This gland contains dark brown structures that could easily appear to be positively stained neurons if included with the TG, as shown in Fig. 8C.

IHC on sectioned ganglia. Ganglia were dehydrated, paraffin embedded, and sectioned according to routine procedures. Blocks were serially sectioned, and a ribbon of three to four consecutive sections was placed on each slide. For analysis of ganglia on day 4 p.i., every other slide (for a total of 15 slides) was examined. For analysis during reactivation, all slides were examined. Deparaffinized sections were incubated for 45 min in anti-HSV-1 antibody (Accurate), biotinylated goat anti-rabbit antibody diluted 1:200 (Vector), and avidin-alkaline phosphatase conjugate (Vector). Antigen-antibody complexes were visualized by using Fast Red chromogen as previously described (17). A rabbit antibody directed against neurofilament 200 (Sigma) was used at a dilution of 1:300, followed by an anti-rabbit-HRP conjugate (Vector) diluted 1:500. The chromogenic substrate VIP (Vector) was used according to the manufacturer's directions to visualize the deposition of anti-neurofilament-HRP complexes.

Cresyl violet staining. Deparaffinized and rehydrated sectioned ganglia were incubated for 5 min in a solution of 10% acetic acid containing 0.5% cresyl violet (Sigma). Sections were then rinsed in distilled H_2O, dehydrated, cleared in xylene, and mounted with Permount (Fisher Scientific). Whole ganglia and sectioned tissue were viewed and photographed under an Olympus BX40 microscope with a digital DP-10 camera.

RESULTS

The purpose of the present study was to test the hypothesis that immune cells infiltrating the TG during the acute stage of ocular HSV infection block reactivation in the ganglion in vivo. The infiltrating cells increase in number in the infected ganglion until 12 to 21 days p.i. and then decrease but remain in low numbers in the ganglion during latency (22, 43). Infiltrating immune cells harvested from infected ganglia on day 14 p.i. have been shown to block reactivation in an ex vivo model (21). If these infiltrating cells have a similar effect in the intact ganglia in vivo, then reactivation should be reduced when the number of infiltrating immune cells is greatest. Traditionally, reactivation has been measured as a "yes" or "no" event based on the detection of infectious virus in the latently infected ganglion or at the body surface. Because studies in the ex vivo model indicated that not only did the infiltrate reduce reactivation (virus production) but it also reduced the number of neurons that expressed lytic viral genes, an assay to detect and quantify the number of neurons in the ganglia expressing lytic viral protein was developed. With this assay, the stage at which the infiltrating cells blocked reactivation could be determined.

Infectious virus in ganglia pre-HS and 22 h post-HS from 9 to 240 days p.i. Mice were inoculated with strain 17syn+ on bilateral corneal surfaces with 10^5 PFU per eye. On days 9, 17, 31, 60, 90, 120, and 240 days p.i., groups of infected animals were either untreated or induced to reactivate by HS (38). After 22 h, both treated and untreated mice were sacrificed and the TG were removed. One ganglion from each mouse was harvested for analysis of infectious virus, and the other ganglion was processed for the detection of lytic viral proteins as described below and in Materials and Methods.

Figure 1A shows the percentage of ganglia positive for infectious virus before and after HS induction. HS has been
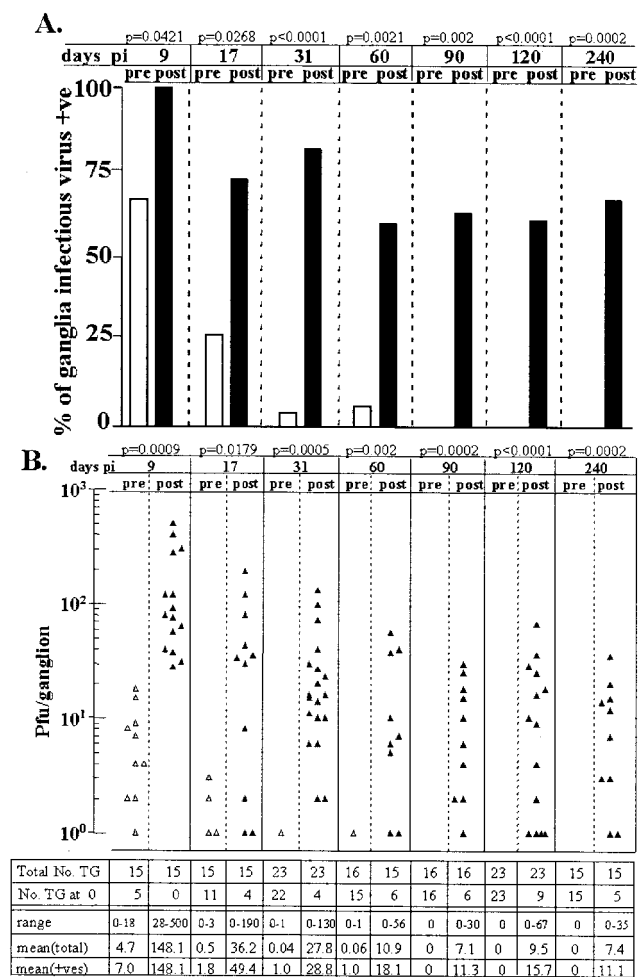
A.

B.

	days pi 9		17		31		60		90		120		240	
	pre	post	pre	post	pre	post	pre	post	pre	post	pre	post	pre	post
Total No. TG	15	15	15	15	23	23	16	15	16	16	23	23	15	15
No. TG at 0	5	0	11	4	22	4	15	6	16	6	23	9	15	5
range	0-18	28-500	0-3	0-190	0-1	0-130	0-1	0-56	0	0-30	0	0-67	0	0-35
mean(total)	4.7	148.1	0.5	36.2	0.04	27.8	0.06	10.9	0	7.1	0	9.5	0	7.4
mean(+ves)	7.0	148.1	1.8	49.4	1.0	28.8	1.0	18.1	0	11.3	0	15.7	0	11.1

FIG. 1. Infectious virus in the TG from 9 to 240 days p.i. pre-HS and 22 h post-HS induction. (A) Bar graph of the percentage of ganglia that were found to be positive for virus. (B) Scattergram of the PFU per ganglion detected. Each symbol represents the PFU in an individual ganglion. Aligned under each scattergram column is the total number of TG in that group, the number of TG at 0 (negative), the range of positive values, the mean of the total TG analyzed, and the mean of the positive (+ve) TG values. The P value (panel A, Fisher exact test; panel B, Student t test [two-tailed]) of the pre- and post-HS values appears at the top of columns for each time point examined. The total number of TG in each group is shown below the scattergram. The P value (A, Fisher exact test; B, Student t test [two-tailed]) of the pre- and post-HS values appears at the top of columns for each time point examined.

shown to induce reactivation (as determined by the production of infectious virus) in the latently infected ganglia (34–39). The timing of peak virus production has been shown to be 22 to 24 h posttreatment (35, 38). Consistent with these previous reports, a significant increase in the percentage of latently infected ganglia containing infectious virus was observed at 22 h post-HS, from ca. 0 to 2% to >60% (P range, <0.0001 to 0.002 [Fisher exact test]). However, at times earlier than 30 days p.i., much greater numbers of ganglia (67% [day 9] and 27% [day 17]) contained one or more PFU prior to induction. The increases in the numbers of ganglia positive for virus after induction on days 9 and 17 p.i. were significant ($P = 0.0421$ and

0.0268, Fisher exact test). This two- to threefold increase was less than the ~20-fold increase observed after 30 days p.i. (Fig. 1A) but reflects only the presence or absence of virus. Evaluating the amount of virus in the ganglia would provide a more complete picture of the changes in lytic activity occurring post-HS. Therefore, the infectious virus titers in the ganglion pre- and postinduction were determined.

Figure 1B is a scattergram of the PFU recovered from each ganglion examined at the time points indicated pre- and post-HS. The total number of ganglia examined at each time point, the number of ganglia negative, and the range and mean of the PFU in the ganglia are presented in a table beneath the scattergram. This analysis revealed that a large increase in infectious virus within the ganglia occurred during the 22 h after induction. At times >30 days p.i., the average PFU/ganglion increased from 0.02 to 13.5 (P range, 0.001 to 0.009 [Student t test, two-tailed]). This burst of infectious virus production in the ganglion was not inhibited at early times p.i., since virus recovered on day 9 p.i. increased from 4.7 to 148.1 PFU by 22 h postinduction and increased from 0.5 to 36.2 PFU on day 17 p.i.

These data demonstrated that HS results in an increase in the infectious virus titer in the TG on days 9 and 17 p.i. This could be due to an increase in the number of neurons producing virus (e.g., reactivation) or an increase in the amount of virus produced by lytically infected cells. Two approaches were utilized to address this question. First, mice inoculated with 17syn+ as described above were treated with ACV from days 6 though 12 p.i. to stop residual lytic viral replication. On day 14, half of these ACV-treated animals were examined without further treatment, and the other half were induced to reactivate by using HS. At 22 h post-HS, both groups were sacrificed, and the TG were removed to determine the infectious virus titers in the individual ganglia. As anticipated, ACV treatment reduced lytic virus to undetectable levels (Fig. 2). At 22 h post-HS, however, there was detectable infectious virus in 72% of the ganglia, with a mean viral titer of 38.2 PFU (range, 0 to 200 PFU) (Fig. 2). These data provide support for the conclusion that the increase in virus is a result of reactivation.

In order to further examine this issue, a second approach was developed to directly examine and quantify the number of viral-protein-expressing cells in the ganglia. To date, there has been no comprehensive quantitative evaluation of the number and type of cells producing the virus and/or viral protein expression over time after inoculation before and after reactivation induction in vivo. This is largely due to the fact that viral protein expression is exceedingly rare during latency and reactivation in vivo. In order to overcome the challenges of this classic "needle in the haystack" situation, an assay was developed that is described below.

Quantitative cell-based "reactivation" assay by WGIHC. A whole-mount labeling system seemed ideally suited to examine and quantify in vivo reactivation of HSV. This type of approach yields an immediate, three-dimensional view of all stained components within the tissue, thereby facilitating the identification and, importantly, the quantification of rare, positively stained cells. Detection of HSV protein during acute infection in whole intestine (9, 10) and cornea (42) has been reported, as have IHC analyses of brain slices, for example (4). These protocols were not suited for quantitative assays of adult
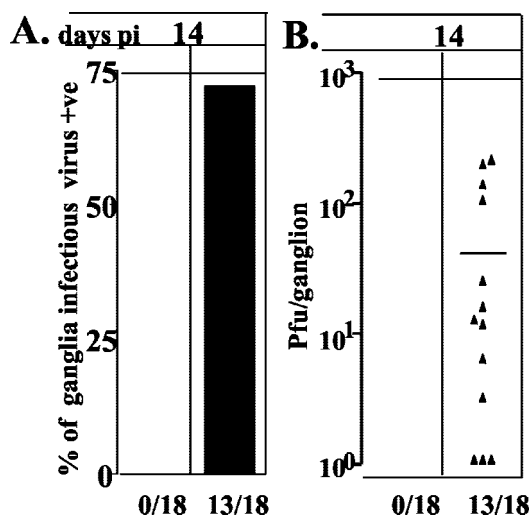
FIG. 2. Infectious virus in the TG on day 14 p.i. of mice pre-HS and 22 h post-HS induction treated with ACV on days 6 to 12 p.i. (A) Percent ganglia in which infectious virus was detected; (B) scattergram showing the number of PFU detected in each virus-positive ganglion.

mouse whole ganglia since penetration of the reagents after these fixation regimens were limited in adult TG (unpublished observation). To our knowledge, there are no previous reports of whole-mount immunolabeling of adult mouse ganglia; however, a procedure specifically adapted for the detection of proteins in the developing mammalian nervous system has been reported (25). This protocol, with the addition of a glucose oxidase blocking procedure (1), worked well for the detection of HSV proteins during acute infection in adult mouse ganglia (Fig. 3).

Assay evaluation: reagent penetration. If reagents did not penetrate through the entire tissue, underestimation of the actual number of viral-protein-expressing neurons would occur. To determine the efficiency of reagent penetration, infected ganglia were first stained by using whole-ganglion IHC. These ganglia were subsequently dehydrated, paraffin embedded, sectioned, and restained by using a chromagenic substrate distinguishable from that used for the whole-ganglion staining. Two experiments were performed. First, ganglia harvested on day 4 of the acute infection were stained for HSV protein by using whole-ganglion IHC. This time point was chosen because the large number of neurons expressing viral proteins in the ganglion at this time point would be predicted to increase the chance of detecting "missed" positives during the restaining process. In the second experiment, ganglia harvested from latently infected mice at 22 h post-HS were utilized. The deposition of a single chromagenic substrate, either Fast Red or diaminobenzidine (brown), could be distinguished from the combined deposition of the substrate products. Thus, HSV protein-containing cells within the tissue not exposed to the IHC reagents during the whole-ganglion staining would be evident as exclusively Fast Red positive after the sectioning and restaining step. The entire thickness of the ganglion tissue blocks was sectioned. The numbers of slides stained in each experiment are given in Materials and Methods. Of the 378 immunolabeled cells examined in day 4 acutely infected ganglia, 376 (99.5%) contained both brown and red precipitate,

indicating that the IHC reagents efficiently penetrated the ganglia. In the second experiment, latently infected ganglia at 22 h post-HS were examined as described above. All of the neurons (i.e., nine of nine) detected in the eight ganglia by IHC of sectioned ganglia were detected during the WGIHC analysis, again confirming that the reagents efficiently penetrated the ganglia. Subsequent staining of the sectioned tissue with an antibody to neurofilament demonstrated that the antigens were not destroyed during the processing. A representative section of latently infected TG harvested at 22 h post-HS and first stained by WGIHG for HSV proteins, followed by restaining after routine embedding and sectioning, is shown in Fig. 4.

To further confirm that the whole-ganglion staining would yield valid quantitative data, the number of neurons expressing viral proteins at 22 h post-HS was determined by using IHC on serially sectioned TG and compared to the number detected by using WGIHC. Ten mice latently infected with 17syn+ were induced to reactivate by using HS (38). At 22 h post-HS, the TG from 10 mice were harvested. One ganglion from each animal was fixed for WGIHC; the second ganglion was fixed in 4% paraformaldehyde, paraffin embedded, and serially sectioned; and all sections were stained for HSV proteins as described previously (38). Note that each group contained equal numbers of right and left ganglia. Examples of viral-protein-expressing neurons from sectioned and whole ganglia are shown in Fig. 5A and B, respectively. Immunostaining was observed exclusively in neurons in both the sectioned and the whole ganglia, a finding consistent with the hypothesis that reactivation is restricted to neurons. In whole ganglia, 70% (7 of 10) of the ganglia contained 1 or more HSV protein-positive neurons, ranging from 1 to 5, with an average of 2.3 neurons/positive ganglion. A total of 12 HSV protein-positive neurons were detected in the sectioned ganglia, a finding somewhat less than the total number of 16 observed in the whole ganglia. The fact that fewer neurons were observed in the sectioned ganglia is consistent with the inevitable loss of some tissue during sectioning, although there was no significant difference between these groups. What was significantly different between the two methods was the amount of labor required to obtain the data; serial sectioning followed by IHC required >10-fold more time than did WGIHC.

Quantification of viral-protein-expressing cells in ganglia from days 9 to 240 p.i. The second of each ganglion pair harvested on days 9, 17, 31, 60, 90, 120, and 240 as described above was processed for WGIHC, and a polyclonal antiserum directed against lytic viral proteins was used to detect viral-protein-expressing cells. The number of viral-protein-positive cells in each ganglion was determined. Since a study examining a large number of ganglia for viral protein expression during latency has not been reported previously, the results are presented here in some detail. During latency (≥31 days p.i.), detection of viral protein was rare, although at 31 days p.i., 17% of the ganglia contained a single positive neuron. This percentage decreased as the time p.i. increased (Fig. 6A). During the ~200 days of latency examined, a total of 92 latently infected noninduced ganglia were analyzed by WGIHC. None contained more than a single viral-protein-positive neuron, and only 6.5% of the ganglia contained a single positive neuron. This means that in a group of latently infected ganglia, ca. 1 ganglionic neuron out of ~350,000 expresses viral protein
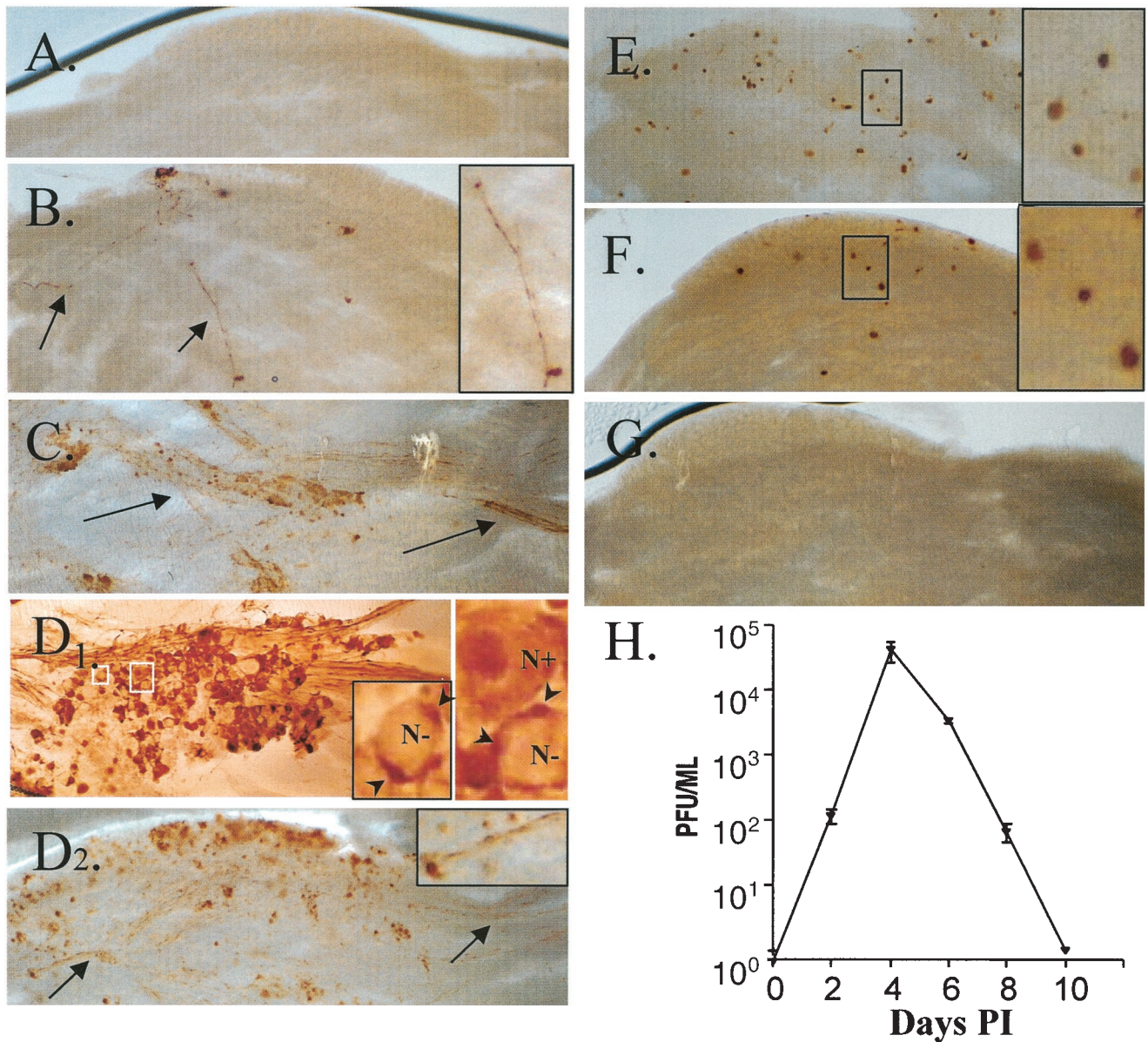
FIG. 3. Photomicrograph series showing representative areas of the TG after WGIHC with an anti-HSV antibody as described in Material and Methods. Viral protein expression is shown over time in the TG of mice after corneal inoculation with HSV type 1 strain 17syn+. (A to D) Representative samples from days 1 to 4 p.i., respectively. (D1 and D2) Images obtained at day 4 p.i., indicating the range of immunostaining observed at this time. The boxed region, shown enlarged to the right of D1, shows a neuron (N−) that is devoid of detectable HSV protein but surrounded by satellite cells (arrowheads) that are positive. N+, neuron positively stained. (E to G) Images representative of days 5, 7, and 30 p.i., respectively. (Insets, E and F) Viral protein was detected in axonal tracts through day 4 (arrows and insets) but was not observed at later times p.i.. (H) Acute viral replication curve.

detectable by WGIHC. Considering that 25% of these neurons would be anticipated to contain HSV genomes (33, 34, 36, 39, 52), viral protein can be detected in <0.001% of latently infected neurons. The percentage of latently infected ganglia in which infectious virus could be detected during latency was similar but less. Only 2 of 93 (2.2%) latently infected noninduced ganglia contained detectable virus and just 1 PFU in each of the positive ganglia. Thus, as generally accepted and reported previously, spontaneous reactivation is rarely detected in the mouse (2, 3, 11, 12, 18, 29, 38, 45, 46, 49, 50, 53). Examination of both parameters in a single study emphasizes

the very strict regulation of not only the production of infectious virus but also the translation of viral proteins during latency.

After 30 days p.i., the percentage of ganglia containing viral-protein-positive neurons increased from an average of 6.5% pre-HS to >60% at 22 h post-HS (P range, <0.0001 to 0.0021 [Fisher exact test]). The average number of viral-protein-positive neurons/ganglion increased from 0.06 to 1.93 (P range, <0.0001 to 0.004 [Student t test, two-tailed]) (Fig. 6). Although there was a trend toward fewer PFU and fewer viral-protein-positive neurons during reactivation with increasing time into
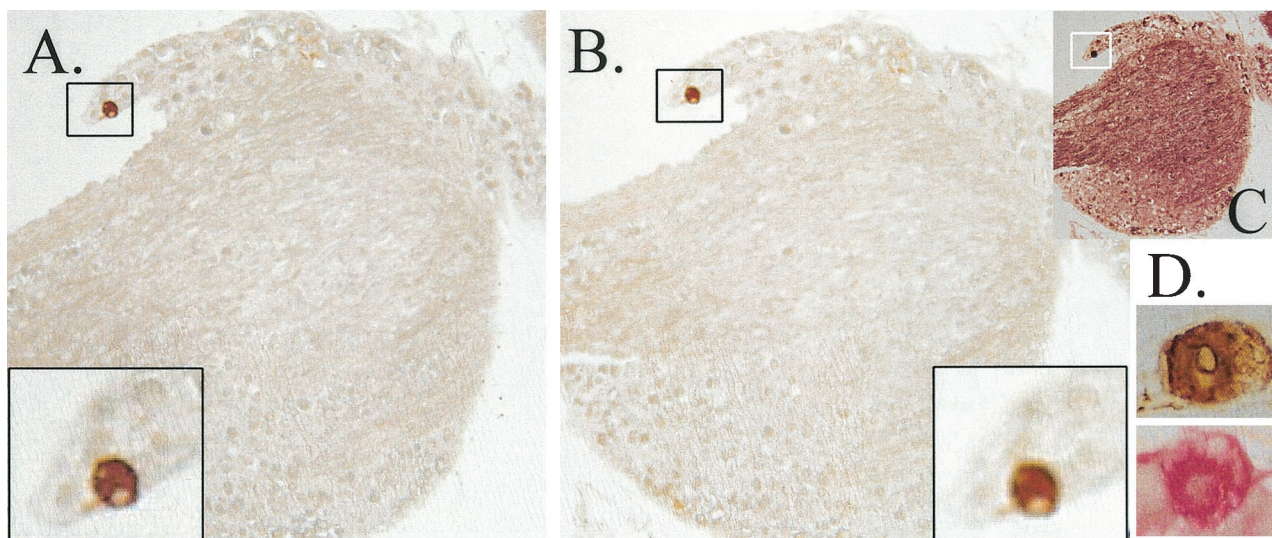
FIG. 4. Analysis of penetration of IHC reagents into the TG. TG were first assayed for viral proteins by using WGIHC. These ganglia were then embedded in paraffin, serially sectioned, and restained by using the anti-HSV antibody and a red chromagenic substrate as detailed in Materials and Methods. (A) Portion of a latently infected TG at 22 h post-HS containing a single viral-protein-positive neuron (box). This neuron was detected during WGIHC. (B) After restaining, no additional viral protein staining was detected. (C) The same section as in panel B after being stained with a neurofilament antibody and VIP (Vector) as the chromagenic substrate, confirming that processing had not destroyed antigenicity of the tissue. (D) Brown (diaminobenzidine)- and red (Fast Red)-stained neurons.

latency, there were no significant differences among the groups.

At earlier times p.i. (days 9 and 17) 100 and 50% of the ganglia, respectively, contained one or more viral-protein-positive neurons (Fig. 6A). At 22 h post-HS, HSV protein-positive neurons were detected in all ganglia (Fig. 6). Again, it is clear that, considering the percentage of ganglia positive without considering the magnitude of the positivity would be misleading. For example, on day 9 p.i., 100% of ganglia were positive for viral-protein-expressing neurons pre- and post-HS. However, the number of positive neurons was 2 to 23 (mean = 11.8) pre-HS, whereas a range of 12 to 70 positive neurons (mean = 38) were detected post-HS. Despite the fact that the same percentage of ganglia were positive, these groups are significantly different ($P < 0.0001$ [Student t test, two-tailed]). Similarly, on day 17, the mean number of HSV-positive neurons per ganglion increases from 2 to 12.3 by 22 h post-HS (Fig. 6B). Inflammatory infiltrate was confirmed to be present in the ganglia at these times (Fig. 6C).

Correlation between infectious virus and viral protein expression. These data provide the first quantitative view of in vivo reactivation in terms of infectious virus production in the ganglia and the number of neurons evidencing lytic gene expression. In Fig. 7, the number of positive ganglia and the magnitude of the positivity are combined in bar graphs of the mean PFU/ganglion (Fig. 7A and C) or mean number of viral-protein-expressing neurons (Fig. 7B and D) pre- and post-HS from days 9 to 240. These data show that there is a consistent parallel between PFU count and viral-protein-positive neurons both pre- and post-HS and that HS induces significant increases in the number of PFU, as well as in the number of positive neurons detected per ganglion at all time points examined p.i., even as early as day 9. Figure 7E shows the plot of the average number of viral-protein-positive neurons per gan-

glion versus the average number of PFU per ganglion at the times between days 9 and 240 p.i. examined. There is a direct correlation between these two parameters over the entire time examined (Pearson r value = 0.99, $P < 0.0001$ [two-tailed]), strongly supporting the notion that the viral-protein-expressing neurons are the source of the virus detected in the ganglion.

Types of cells expressing viral proteins during latency and reactivation. In addition to the quantitative data presented above, WGIHC allows a view of the morphology (size and shape) of the immunolabeled cells and thereby can provide insight into the type and metabolic state of the cells, as well as into the distribution of the label within the cells. On days 9 and 17 p.i., the cells positive for viral proteins pre HS and post-HS are universally neurons (Fig. 6C). A time course of protein expression in the TG from days 0 to 9 p.i. shows that neuronal and nonneuronal cells express viral proteins up through days 5 and 6. After this time, the number of positive cells declines dramatically and only neurons are positive. Figure 3 shows staining for viral proteins on day 4 p.i.

In the latently infected ganglia examined in the present study, a total of 228 cells expressing viral protein pre- and post-HS were observed. On the basis of morphology, all of these viral-protein-positive cells were neurons. As shown in Fig. 3, it is reasonable to use size and shape as criteria to distinguish neurons from support cells in the TG. In the 92 uninduced latently infected ganglia examined, 6 neurons expressing HSV proteins were detected. Several of these neurons showed evidence of disintegration (an example is shown in Fig. 8B). Presumably, these cells had undergone reactivation and were in the process of being destroyed (7, 38, 40, 44). A total of 112 latently infected ganglia were examined for viral protein expression at 22 h post-HS, the time of peak infectious virus production during reactivation in the TG. The vast majority of the 228 neurons identified on the basis of viral protein expres-
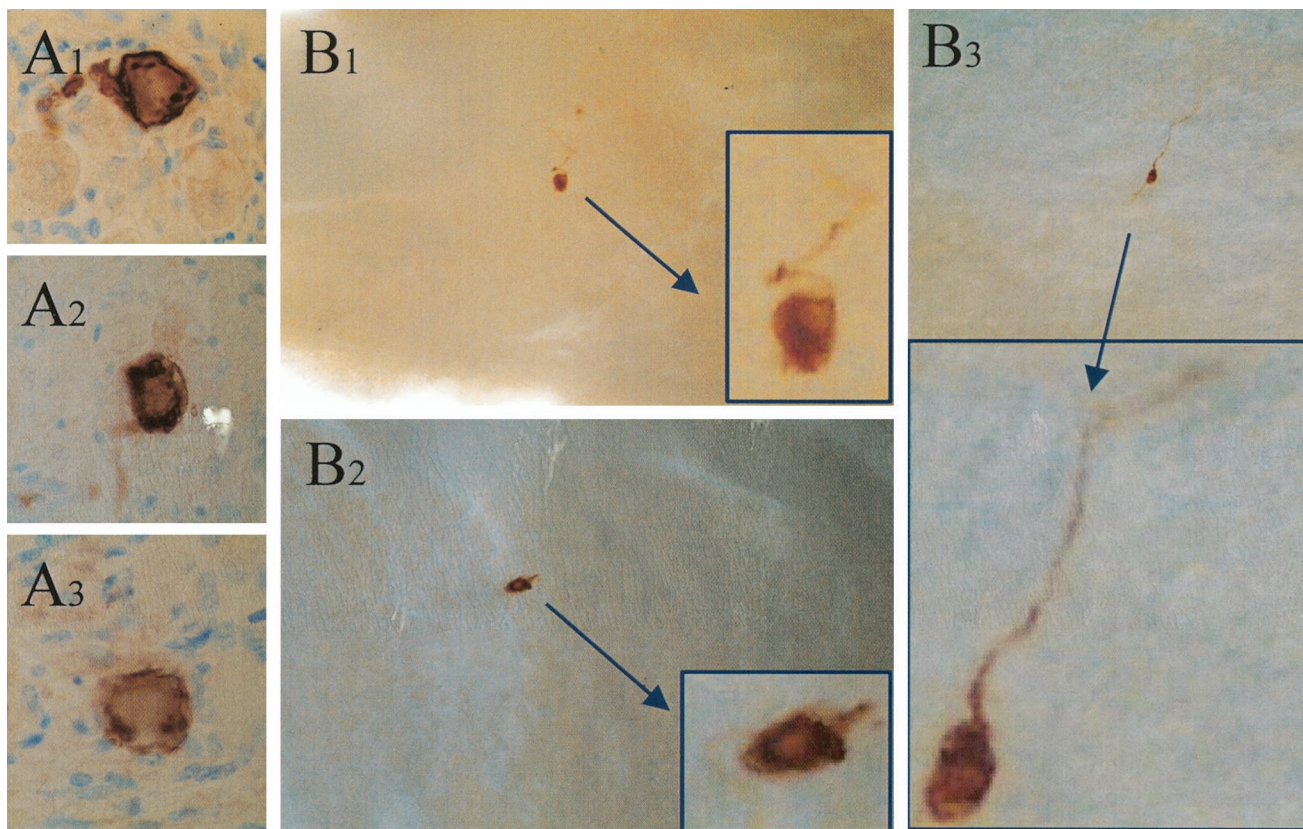
FIG. 5. Analysis of viral protein expression in TG of latently infected mice at 22 h post-HS by using an anti-HSV antibody on serially sectioned ganglia (A1 to A3) or whole ganglia (B1 to B3). Insets show higher magnifications of immunostained neurons.

sion as having entered lytic-phase transcription at this time appeared intact (Fig. 8A). In many cases, axons were labeled, confirming that the labeled cell bodies were neurons and indicative of axonal transport of viral proteins and/or virus (Fig. 8A). We reasoned that if the disintegrating neurons observed during latency represented the resolution of a "spontaneous" reactivation event, these profiles would increase at times beyond 22 h post-HS when reactivation in the ganglia was being shut off. In order to test this, ganglia were examined at 42 h post-HS for the expression of viral proteins by using WGIHC. At this time point post-HS, 70% (7 of 10) of the viral-protein-positive neurons observed in 20 ganglia appeared to be neurons in various stages of disintegration (Fig. 8B), a finding consistent with the idea that these were indeed neurons in the end stages of reactivation and that neurons do not survive this process.

DISCUSSION

Understanding the mechanisms that regulate reactivation of HSV from latency remains a major goal in the field of HSV pathogenesis. The interactions between the virus and the host immune system are undoubtedly important facets of this process. Ultimately, prevention or reduction of infection and reactivation will require a greater understanding of these interactions. Recent studies have indicated that the immune cells infiltrating into the TG during acute infection have the ability

to block viral reactivation in an ex vivo model (21). The relevance of these ex vivo observations to reactivation in vivo has not been previously tested. In the present study, the ability of the ex vivo system to accurately model immune function during reactivation in vivo was examined. In the ex vivo model, infiltrates isolated from infected TG at 14 days p.i. blocked reactivation of virus in a culture setting, but immune cells isolated at day 34 p.i. lost this ability (21). These findings led to the hypothesis that either the number of immune cells or the environment in the ganglia at earlier times p.i. maintains the immune cells in an activated state (21). If this is the case, then reactivation should be reduced or blocked in vivo at early times p.i., the time that the infiltrate within the TG effectively blocked reactivation ex vivo (21). Our data indicate that in vivo, despite abundant infiltrating immune cells in the TG, reactivation is not blocked at early times p.i. Therefore, although the inflammatory cells in the ganglia have the ability to block infectious virus production when added to cultures ex vivo, increased numbers of infiltrating lymphocytes in the ganglia do not appear to effectively inhibit or reduce reactivation in vivo.

There are a number of potential explanations for the inability of the ex vivo model to predict function in the in vivo setting. Most obvious and perhaps most significant is the difference in physical cellular environments between the two model systems. In the ex vivo model, the context of the latently infected neurons within the ganglia is completely disrupted, as
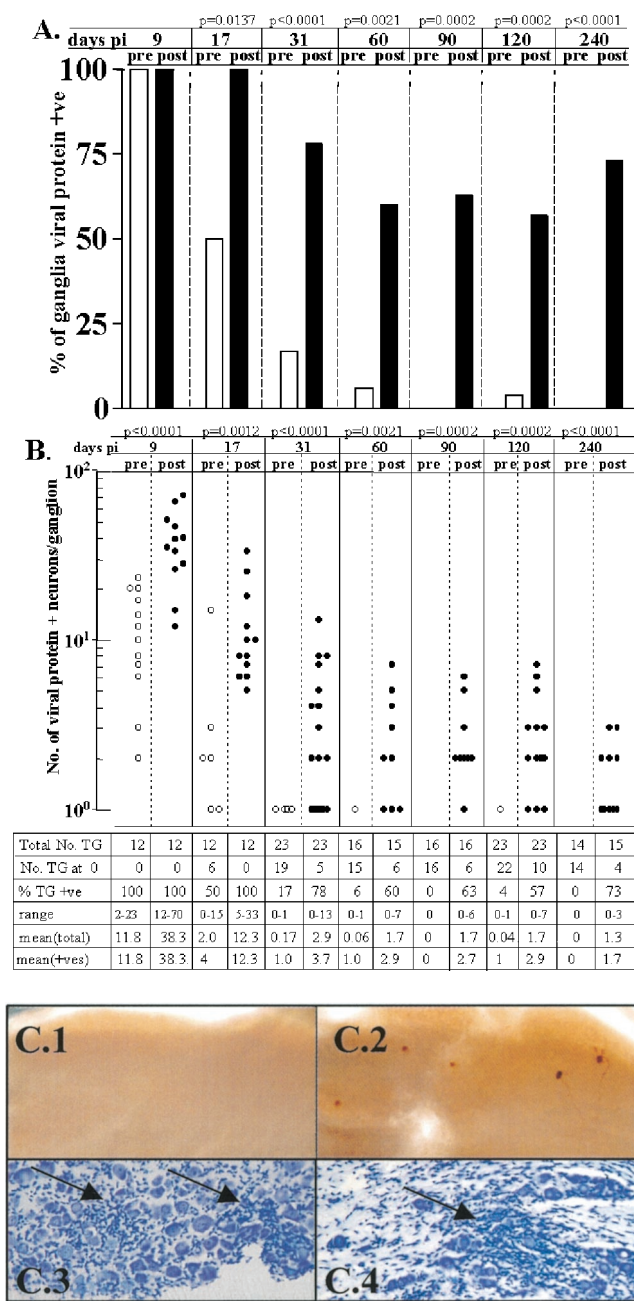
FIG. 6. Viral protein expression in the TG from 9 to 240 days p.i. before and 22 h post-HS induction. (A) Bar graph of the percentage of ganglia that were found to be positive for viral proteins by using WGIHC. (B) Scattergram of the number of positive neurons per ganglion detected. Each symbol represents the value obtained for an individual ganglion. Aligned under each scattergram column is the total number of TG in that group, the number of TG at 0 (negative), the range of positive values, the mean of the total TG analyzed, and the mean of the positive (+ve) TG values. The *P* value (panel A, Fisher exact test; panel B, Student *t* test [two-tailed]) of the pre- and post-HS values appears at the top of columns for each time point examined. (C) Example of latently infected ganglia on day 17 pre-HS induction (C.1) and 22 h post-HS induction (C.2). These TG were subsequently embedded and stained with cresyl violet. Areas of inflammatory infiltrate were present before (C.3) and after induction (C.4) (arrows).

is the context of the inflammatory cells isolated from the TG and added back to the cultured dissociated neurons. Axotomy of the ganglia alone induces many metabolic changes in the neurons, including apoptosis (27, 54). Combined with removal of the ganglia from the animal and enzymatic stripping of the neurons from supporting cells, the setup of the ex vivo model is likely to result in a neuronal population that diverges dramatically from the physiological parameters defining neurons during latency and reactivation in vivo. Similarly, inflammatory cell function is context driven. Removal of the immune cells from the ganglia eliminates exposure to the signals within this environment. Other differences include the mouse strain (i.e., BALB/c versus Swiss-Webster) and the virus strain (RE versus 17syn+) utilized. Although these differences cannot be ignored, in our experience the acute ocular infection and in vivo reactivation are very similar in these two strains of mice with strain 17syn+ (unpublished observations). RE is a virulent strain that would be expected to behave like the 17syn+ strain.

The central feature of the assay presented here for HSV gene expression is that the IHC is performed on the whole ganglia. This not only eliminates labor-intensive serial sectioning and unavoidable associated tissue loss but also provides for immediate and complete visualization of expression in the ganglia. The types of cells being stained and their spatial relationships can be determined. This approach has been utilized extensively on embryos for mapping gene expression during development (5, 15, 51) but, to our knowledge, has not previously been utilized on adult TG. When applied to the analysis of latent and reactivating ganglia, the advantages are quite clear. As an example, consider that in this report more than 230 ganglia were analyzed for HSV protein expression from day 9 though day 240 p.i. Using standard IHC on serial sectioned tissue (note that serial sectioning is essential for detecting the rare viral-protein-expressing cells), a minimum of 10,000 ganglion profiles would have to be processed and individually evaluated. In contrast, the viral protein expression pattern of the 20,000 or so neurons in an entire ganglion can be observed in one view by using WGIHC. This is especially significant when it is important to accurately quantify rare events. These same advantages are provided by whole-mount staining of reporter mutants or promoter/reporter-containing transgenic mice, and we and others have found this approach to be useful for certain latency and reactivation studies (16, 23, 26, 37, 41). However, the use of promoter reporter mutants as surrogate markers for protein expression requires demonstration that expression of the reporter and the protein coincide. Certainly, there is no scientific basis for assuming that all promoter reporter mutants will reflect expression of the relevant protein under all physiological conditions. Using WGIHC, the uncertainty of fidelity between reporter expression and actual protein production can now be obviated by direct detection of the relevant protein.

Viral protein was detected in about 1 of 17 uninduced latently infected mouse ganglia, and only one viral-protein-expressing neuron was observed in each of these ganglia. Are these neurons undergoing reactivation or merely expressing a subset of viral proteins? Two lines of evidence indicate that these neurons are indeed undergoing reactivation. First, in the parallel analysis of infectious virus, 1 in 30 latent ganglia contained detectable albeit very low levels of virus, a finding con-
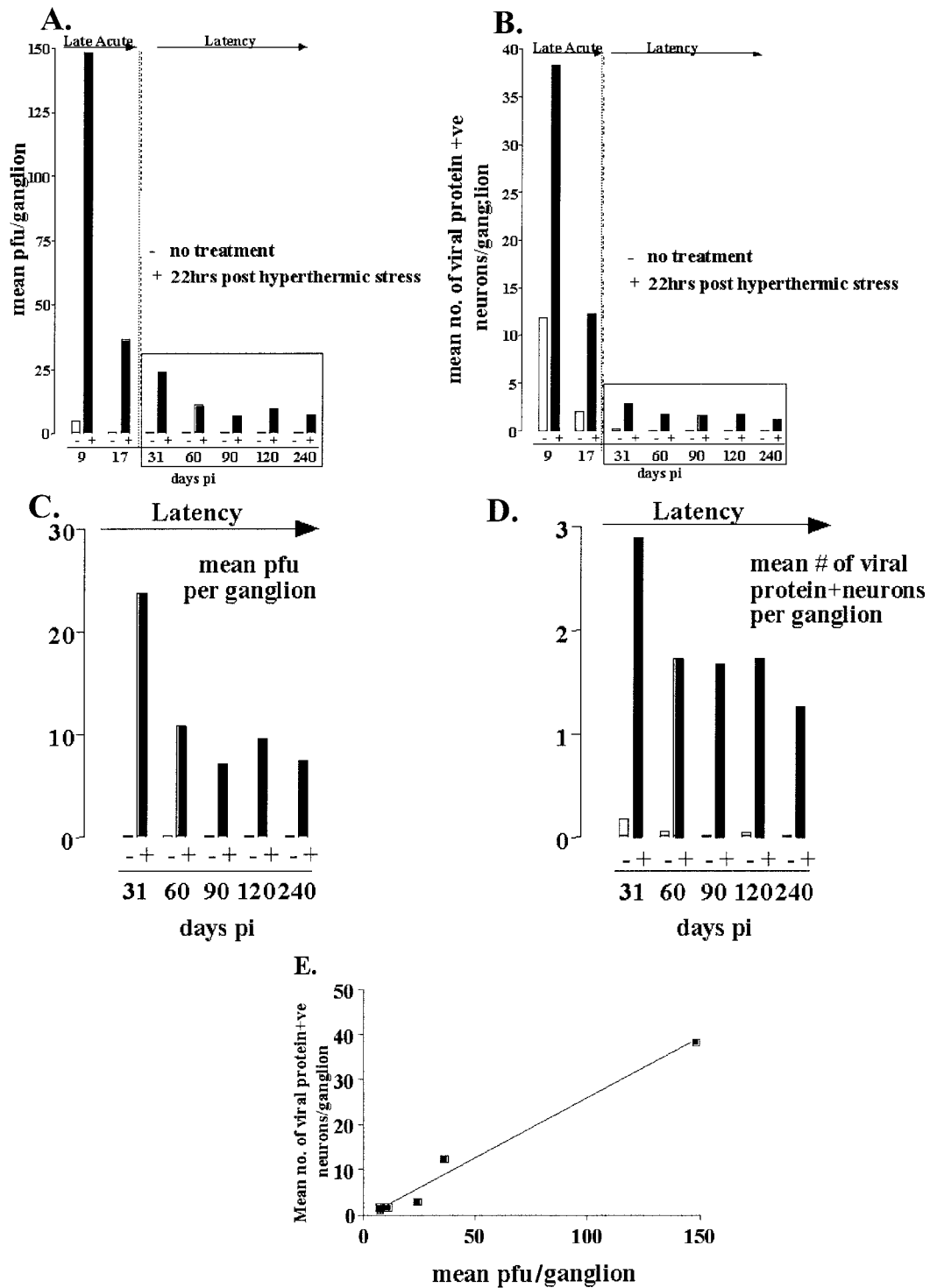
FIG. 7. Graphic representation of mean PFU per TG (A) and mean number of viral-protein-expressing neurons per TG (B) pre-HS and 22 h post-HS in mice from 9 to 240 days p.i. (C and D) The results from days 31 to 240 p.i. are shown on expanded scales. (E) Correlation of 0.99 (Pearson r value, $P < 0.0001$) was found between the mean PFU per ganglion and the mean number of viral-protein-positive neurons per ganglion at 22 h post-HS from days 9 to 240 p.i.

sistent with the hypothesis that the protein-expressing neurons are undergoing reactivation. Second, examination of latently infected ganglia by using the WGIHC reveals the presence of viral-protein-positive areas that appear to be neurons at vari-

ous stages of destruction (Fig. 8), suggesting a low rate of ongoing reactivation in the latent ganglia. Based on the survey of 92 uninduced latently infected ganglia examined in the present study and estimating the number of latently infected
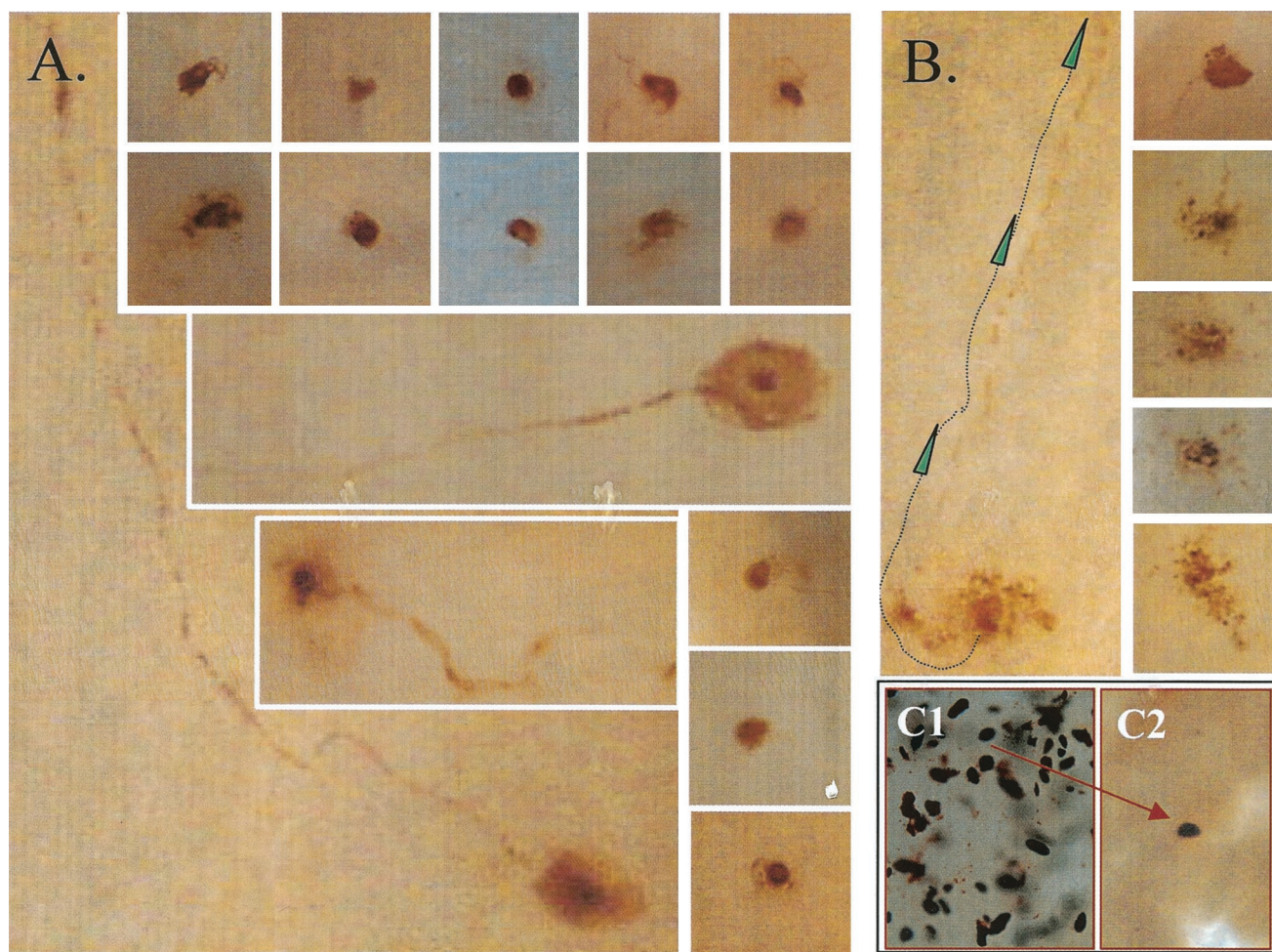
FIG. 8. Photomicrographs of viral-protein-expressing neurons post-HS of latently infected animals. (A) Examples of neurons expressing viral proteins 22 h post-HS. Note that viral proteins can often be detected in the axon, as well as in the cell body. (B) Ganglia examined at 48 h post-HS contained viral-protein-positive neurons that appeared to be undergoing destruction. The presence of viral protein in the axon confirms that this cell is a neuron. (C) Care must be taken to avoid pieces of lacrimal gland during the dissection of the TG (see Materials and Methods). These glands contain very dark brown or black structures (C1), as shown here, that can be misinterpreted as stained neurons if allowed to contaminate the ganglion preparation (C2).

neurons to be ~6,000 per ganglion (33), it can be estimated that at any given time one latent neuron out of every 90,000 latent neurons (0.001%) is undergoing reactivation.

In a recent report, one viral-protein-positive neuron in 10 latently infected ganglia was estimated from IHC analysis of sectioned material harvested from mice between 37 and 47 days p.i. (7). Although this 10% estimate is higher than our average figure of 6.5%, this result can be explained if the time of examination is considered. In our study, at 31 days p.i., 17% of uninduced latently infected ganglia were found to be positive, whereas only 6% of ganglia were positive on day 60. The percentage of positive ganglia among uninduced animals decreased from 17% on day 31 to 0% on day 240 p.i., suggesting that the level of spontaneous reactivation decreases as the amount of time p.i. increases. In the earlier study, Feldman et al. (7) concluded that 1 in 5,000 latently infected neurons is expressing lytic viral transcripts compared to our estimate of 1 in 90,000. This difference stems from the use of latency-associated transcript-positive sites (detected by in situ hybridiza-

tion) by Feldman et al. as an estimate of latently infected neurons in the ganglion. By in situ hybridization, latency-associated transcripts can be detected in only a subset of latently infected neurons, and thus this measure underestimates the number of neurons containing the latent viral genome (32). In the present study, 92 ganglia were examined and the number of latently infected neurons was estimated based on detection of the viral genome by using single neuron PCR as described previously (33).

The parallel analyses of infectious virus and viral-protein-expressing cells in reactivating ganglia at the time of peak virus production in the ganglia are the first such study reported. The results provide compelling data that the viral-protein-expressing cells generate the infectious virus. In other words, these are the cells undergoing reactivation. Demonstration that these cells contain virion particles will be required for more definitive proof, and this is ongoing. However, the direct correlation (Pearson r value = 0.99, P < 0.0001) between the amount of infectious virus produced and the increase in the number of

viral-protein-expressing cells strongly indicates that using an antibody directed against HSV lytic viral proteins marks cells undergoing viral reactivation. The modest amount of infectious virus produced during reactivation in the ganglia has been reported previously (6, 34, 38) and is consistent with findings here. Including all experiments, we observed 222 cells expressing viral protein at 22 h post-HS in 112 latently infected ganglia. Examination of this large population allows us to draw some firm conclusions about reactivation in vivo in this mouse model. First, only cells morphologically distinguishable as neurons were found to express viral proteins. Thus, consistent with the neuron being the site of latency in the ganglion, reactivation in vivo appears to be restricted to neurons, and whether reactivation is restricted to certain type(s) of neurons is currently under investigation. Second, there was no evidence of lateral spread of virus to neighboring cells, indicating that in the ganglion in vivo the release of infectious virus is highly controlled. Third, the ability to view the distribution of selected proteins within neurons and associated axons and/or dendrites should be valuable for addressing certain questions of transport during reactivation in vivo. In the present study, viral proteins in neurites leading from the periphery to the ganglion and the ganglion to the central nervous system were abundant during the acute stage of infection. In contrast, during reactivation, viral proteins were detected almost exclusively in the neuronal process directed toward the body surface (compare Fig. 1 and 8). Fourth, a portion of the viral-protein-expressing neurons observed in latently infected ganglia (two of six) showed evidence of disintegration (Fig. 8); this number increased to 70% at 42 h post-HS (Fig. 8), further supporting the notion that reactivating neurons do not survive.

ACKNOWLEDGMENTS

REFERENCES

1. **Bauer, D., and R. Tampe.** 2002. Herpes viral proteins blocking the transporter associated with antigen processing TAP: from genes to function and structure. Curr. Top. Microbiol. Immunol. **269:**87–99.
2. **Blue, W. T., R. D. Winland, D. G. Stobbs, D. F. Kirksey, and R. E. Savage.** 1981. Effects of adenosine monophosphate on the reactivation of latent herpes simplex virus type 1 infections of mice. Antimicrob. Agents Chemother. **20:**547–548.
3. **Blyth, W. A., T. J. Hill, H. J. Field, and D. A. Harbour.** 1976. Reactivation of herpes simplex virus infection by ultraviolet light and possible involvement of prostaglandins. J. Gen. Virol. **33:**547–550.
4. **Card, J. P., P. Levitt, and L. W. Enquist.** 1998. Different patterns of neuronal infection after intracerebral injection of two strains of pseudorabies virus. J. Virol. **72:**4434–4441.
5. **Dent, J. A., A. G. Polson, and M. W. Klymkowsky.** 1989. A whole-mount immunocytochemical analysis of the expression of the intermediate filament protein vimentin in *Xenopus*. Development **105:**61–74.
6. **Fawl, R. L., and B. Roizman.** 1993. Induction of reactivation of herpes simplex virus in murine sensory ganglia in vivo by cadmium. J. Virol. **67:**7025–7031.
7. **Feldman, L. T., A. R. Ellison, C. C. Voytek, L. Yang, P. Krause, and T. P. Margolis.** 2002. Spontaneous molecular reactivation of herpes simplex virus type 1 latency in mice. Proc. Natl. Acad. Sci. USA **99:**978–983.
8. **Fields, B. N., D. M. Knipe, and P. M. Howley.** 1996. Fields virology, 3rd ed. Lippincott-Raven Publishers, Philadelphia, Pa.
9. **Gesser, R. M., and S. C. Koo.** 1996. Oral inoculation with herpes simplex virus type 1 infects enteric neuron and mucosal nerve fibers within the gastrointestinal tract in mice. J. Virol. **70:**4097–4102.
10. **Gesser, R. M., T. Valyi-Nagy, N. W. Fraser, and S. M. Altschuler.** 1995. Oral inoculation of SCID mice with an attenuated herpes simplex virus-1 strain causes persistent enteric nervous system infection and gastric ulcers without direct mucosal infection. Lab. Investig. **73:**880–889.
11. **Hill, T. J., W. A. Blyth, and D. A. Harbour.** 1982. Recurrent herpes simplex in mice: topical treatment with acyclovir cream. Antiviral Res. **2:**135–146.
12. **Hill, T. J., W. A. Blyth, and D. A. Harbour.** 1978. Trauma to the skin causes recurrence of herpes simplex in the mouse. J. Gen. Virol. **39:**21–28.
13. **Keadle, T. L., K. A. Laycock, J. K. Miller, K. K. Hook, E. D. Fenoglio, M. Francotte, M. Slaoui, P. M. Stuart, and J. S. Pepose.** 1997. Efficacy of a recombinant glycoprotein D subunit vaccine on the development of primary and recurrent ocular infection with herpes simplex virus type 1 in mice. J. Infect. Dis. **176:**331–338.
14. **Keadle, T. L., L. A. Morrison, J. L. Morris, J. S. Pepose, and P. M. Stuart.** 2002. Therapeutic immunization with a virion host shutoff-defective, replication-incompetent herpes simplex virus type 1 strain limits recurrent herpetic ocular infection. J. Virol. **76:**3615–3625.
15. **Klymkowsky, M. W., and J. Hanken.** 1991. Whole-mount staining of *Xenopus* and other vertebrates. Methods Cell Biol. **36:**419–441.
16. **Lachmann, R. H., M. Sadarangani, H. R. Atkinson, and S. Efstathiou.** 1999. An analysis of herpes simplex virus gene expression during latency establishment and reactivation. J. Gen. Virol. **80:**1271–1282.
17. **Larsson, L.-I.** 1988. Immunocytochemistry: theory and practice. CRC Press, Inc., Boca Raton, Fla.
18. **Laycock, K. A., S. F. Lee, R. H. Brady, and J. S. Pepose.** 1991. Characterization of a murine model of recurrent herpes simplex viral keratitis induced by ultraviolet B radiation. Investig. Ophthalmol. Vis. Sci. **32:**2741–2746.
19. **Leib, D. A.** 2002. Counteraction of interferon-induced antiviral responses by herpes simplex viruses. Curr. Top. Microbiol. Immunol. **269:**171–185.
20. **Liu, T., K. M. Khanna, B. N. Carriere, and R. L. Hendricks.** 2001. Gamma interferon can prevent herpes simplex virus type 1 reactivation from latency in sensory neurons. J. Virol. **75:**11178–11184.
21. **Liu, T., K. M. Khanna, X. Chen, D. J. Fink, and R. L. Hendricks.** 2000. CD8+ T cells can block herpes simplex virus type 1 (HSV-1) reactivation from latency in sensory neurons. J. Exp. Med. **191:**1459–1466.
22. **Liu, T., Q. Tang, and R. L. Hendricks.** 1996. Inflammatory infiltration of the trigeminal ganglion after herpes simplex virus type 1 corneal infection. J. Virol. **70:**264–271.
23. **Loiacono, C. M., R. Myers, and W. J. Mitchell.** 2002. Neurons differentially activate the herpes simplex virus type 1 immediate-early gene ICP0 and ICP27 promoters in transgenic mice. J. Virol. **76:**2449–2459.
24. **Lubinski, J. M., M. Jiang, L. Hook, Y. Chang, C. Sarver, D. Mastellos, J. D. Lambris, G. H. Cohen, R. J. Eisenberg, and H. M. Friedman.** 2002. Herpes simplex virus type 1 evades the effects of antibody and complement in vivo. J. Virol. **76:**9232–9241.
25. **Luque, J. M., W. B. Adams, and J. G. Nicholls.** 1998. Procedures for whole-mount immunohistochemistry and in situ hybridization of immature mammalian CNS. Brain Res. Brain Res. Protoc. **2:**165–173.
26. **Margolis, T. P., F. Sedarati, A. T. Dobson, L. T. Feldman, and J. G. Stevens.** 1992. Pathways of viral gene expression during acute neuronal infection with HSV-1. Virology **189:**150–160.
27. **McKay Hart, A., T. Brannstrom, M. Wiberg, and G. Terenghi.** 2002. Primary sensory neurons and satellite cells after peripheral axotomy in the adult rat: time course of cell death and elimination. Exp. Brain Res. **142:**308–318.
28. **Mester, J. C., T. A. Twomey, E. T. Tepe, and D. I. Bernstein.** 1999. Immunity induced by DNA immunization with herpes simplex virus type 2 glycoproteins B and C. Vaccine **18:**875–883.
29. **Mitchell, W. J., P. Gressens, J. R. Martin, and R. DeSanto.** 1994. Herpes simplex virus type 1 DNA persistence, progressive disease and transgenic immediate early gene promoter activity in chronic corneal infections in mice. J. Gen. Virol. **75:**1201–1210.
30. **Nesburn, A. B., R. L. Burke, H. Ghiasi, S. M. Slanina, and S. L. Wechsler.** 1998. A therapeutic vaccine that reduces recurrent herpes simplex virus type 1 corneal disease. Investig. Ophthalmol. Vis. Sci. **39:**1163–1170.
31. **Preston, C. M.** 2000. Repression of viral transcription during herpes simplex virus latency. J. Gen. Virol. **81:**1–19.
32. **Ramakrishnan, R., P. L. Poliani, M. Levine, J. C. Glorioso, and D. J. Fink.** 1996. Detection of herpes simplex virus type 1 latency-associated transcript expression in trigeminal ganglia by in situ reverse transcriptase PCR. J. Virol. **70:**6519–6523.
33. **Sawtell, N. M.** 1997. Comprehensive quantification of herpes simplex virus latency at the single-cell level. J. Virol. **71:**5423–5431.
34. **Sawtell, N. M.** 1998. The probability of in vivo reactivation of herpes simplex virus type 1 increases with the number of latently infected neurons in the ganglia. J. Virol. **72:**6888–6892.
35. **Sawtell, N. M., D. I. Bernstein, and L. R. Stanberry.** 1999. A temporal analysis of acyclovir inhibition of induced herpes simplex virus type 1 In vivo reactivation in the mouse trigeminal ganglia. J. Infect. Dis. **180:**821–823.
36. **Sawtell, N. M., D. K. Poon, C. S. Tansky, and R. L. Thompson.** 1998. The latent herpes simplex virus type 1 genome copy number in individual neurons is virus strain specific and correlates with reactivation. J. Virol. **72:**5343–5350.
37. **Sawtell, N. M., and R. L. Thompson.** 1992. Herpes simplex virus type 1 latency-associated transcription unit promotes anatomical site-dependent establishment and reactivation from latency. J. Virol. **66:**2157–2169.
38. **Sawtell, N. M., and R. L. Thompson.** 1992. Rapid in vivo reactivation of

herpes simplex virus in latently infected murine ganglionic neurons after transient hyperthermia. J. Virol. **66:**2150–2156.

39. **Sawtell, N. M., R. L. Thompson, L. R. Stanberry, and D. I. Bernstein.** 2001. Early intervention with high-dose acyclovir treatment during primary herpes simplex virus infection reduces latency and subsequent reactivation in the nervous system in vivo. J. Infect. Dis. **184:**964–971.

40. **Shimeld, C., D. L. Easty, and T. J. Hill.** 1999. Reactivation of herpes simplex virus type 1 in the mouse trigeminal ganglion: an in vivo study of virus antigen and cytokines. J. Virol. **73:**1767–1773.

41. **Shimeld, C., S. Efstathiou, and T. Hill.** 2001. Tracking the spread of a *lacZ*-tagged herpes simplex virus type 1 between the eye and the nervous system of the mouse: comparison of primary and recurrent infection. J. Virol. **75:**5252–5262.

42. **Shimeld, C., S. J. Lewkowicz-Moss, K. M. Lipworth, T. J. Hill, W. A. Blyth, and D. L. Easty.** 1986. Antigens of herpes simplex virus in whole corneal epithelial sheets from mice. Arch. Ophthalmol. **104:**1830–1834.

43. **Shimeld, C., J. L. Whiteland, S. M. Nicholls, E. Grinfeld, D. L. Easty, H. Gao, and T. J. Hill.** 1995. Immune cell infiltration and persistence in the mouse trigeminal ganglion after infection of the cornea with herpes simplex virus type 1. J. Neuroimmunol. **61:**7–16.

44. **Shimeld, C., J. L. Whiteland, N. A. Williams, D. L. Easty, and T. J. Hill.** 1996. Reactivation of herpes simplex virus type 1 in the mouse trigeminal ganglion: an in vivo study of virus antigen and immune cell infiltration. J. Gen. Virol. **77:**2583–2590.

45. **Speck, P. G., and A. Simmons.** 1991. Divergent molecular pathways of productive and latent infection with a virulent strain of herpes simplex virus type 1. J. Virol. **65:**4001–4005.

46. **Spivack, J. G., and N. W. Fraser.** 1987. Detection of herpes simplex virus type 1 transcripts during latent infection in mice. J. Virol. **61:**3841–3847.

47. **Stanberry, L. R., R. Burke, and M. G. Myers.** 1988. Herpes simplex virus glycoprotein treatment of recurrent genital herpes. J. Infect. Dis. **157:**156–163.

48. **Stanberry, L. R., C. J. Harrison, D. I. Bernstein, R. L. Burke, R. Shukla, G. Ott, and M. G. Myers.** 1989. Herpes simplex virus glycoprotein immunotherapy of recurrent genital herpes: factors influencing efficacy. Antiviral Res. **11:**203–214.

49. **Steiner, I., N. Mador, I. Reibstein, J. G. Spivack, and N. W. Fraser.** 1994. Herpes simplex virus type 1 gene expression and reactivation of latent infection in the central nervous system. Neuropathol. Appl. Neurobiol. **20:**253–260.

50. **Stevens, J. G., and M. L. Cook.** 1971. Latent herpes simplex virus in spinal ganglia of mice. Science **173:**843–845.

51. **Tautz, D., and C. Pfeifle.** 1989. A non-radioactive in situ hybridization method for the localization of specific RNAs in *Drosophila* embryos reveals translational control of the segmentation gene hunchback. Chromosoma **98:**81–85.

52. **Thompson, R. L., and N. M. Sawtell.** 1997. The herpes simplex virus type 1 latency-associated transcript gene regulates the establishment of latency. J. Virol. **71:**5432–5440.

53. **Tullo, A. B., C. Shimeld, W. A. Blyth, T. J. Hill, and D. L. Easty.** 1982. Spread of virus and distribution of latent infection following ocular herpes simplex in the non-immune and immune mouse. J. Gen. Virol. **63:**95–101.

54. **Weishaupt, J. H., and M. Bahr.** 2001. Degeneration of axotomized retinal ganglion cells as a model for neuronal apoptosis in the central nervous system: molecular death and survival pathways. Restor. Neurol. Neurosci. **19:**19–27.